

Aromatase Excess Syndrome

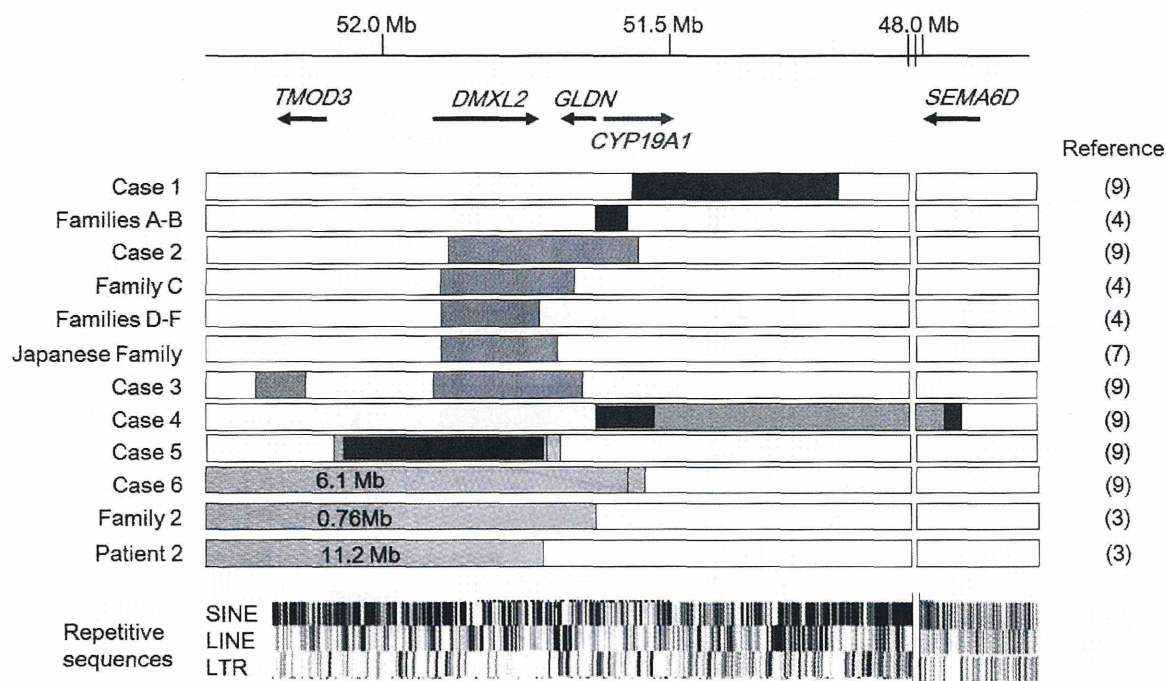


Figure 1: Schematic representation of the 12 genomic rearrangements identified in patients with AEXS (modified from reference #9). Physical distance (in Mb) from the 15p telomere is indicated at the top. Genomic position refers to Human Genome Database (hg19, build 37). The arrows indicate the position and transcriptional direction of CYP19A1 and its neighboring genes (5'>3'). Only genes flanking the fusion junctions are shown. The white areas indicate copy-number neutral regions, and the red, gray, and green areas indicate duplications, deletions, and inversions, respectively. The inversions of family 2 and patient 2 may be complex rearrangements, because copy-number analyses have not been performed for these cases. The presence or absence of repetitive sequences is analyzed using UCSC genome browser (<http://genome.ucsc.edu/>).

AEXS is caused by overexpression of CYP19A1 due to submicroscopic genomic rearrangements involving CYP19A1 and/or its flanking regions. (2-4,7,9) These rearrangements enhance CYP19A1 expression by copy-number gain of this gene or by cryptic use of constitutively active promoters of neighboring genes. The clinical severity of AEXS depends primarily on the type of the rearrangement. This article provides an overview of the molecular basis and clinical manifestations of AEXS.

Molecular Basis of AEXS

AEXS is an autosomal dominant disorder resulting from heterozygous genomic rearrangements at 15q21. (8) To date, 12 types of submicroscopic rearrangements, i.e.,

two simple duplications, four simple deletions, two simple inversions, and four complex rearrangements, have been identified in patients with AEXS. (2-4,7,9) (Figure 1) Of these, two duplications encompass the entire coding exons and/or part of the promoter region of CYP19A1, and are therefore likely to increase the transcriptional efficiency of this gene. (Figure 2) The remaining rearrangements are known or predicted to create chimeric genes consisting of coding exons of CYP19A1 and promoter-associated exons of neighboring genes. (Figure 2) Six widely-expressed genes, DMXL2, CGNL1, TLN2, MAPK6, SEMA6D, and TMOD3, provide cryptic promoters for CYP19A1. Thus, AEXS is a unique example of a congenital disorder caused by gene overexpression due to various genomic rearrangements.

The identification of several submicroscopic rearrangements at 15q21 in patients with AEXS suggests that this region may be a hotspot for genomic abnormalities. (9) In this context, structural alterations in the genome are known to be generated through various mechanisms such as non-allelic homologous recombination (NAHR), non-homologous end-joining (NHEJ), and replication-based error (RBE). (10-13) NAHR results from unequal crossover between two homologous sequences, NHEJ occurs as a result of double-strand DNA breakage and subsequent ligation of the two broken DNA ends, and RBE is caused by aberrant template-switching during replication. Previous studies of patients with AEXS have revealed that multiple mechanisms are involved in the development of rearrangements at

Aromatase Excess Syndrome

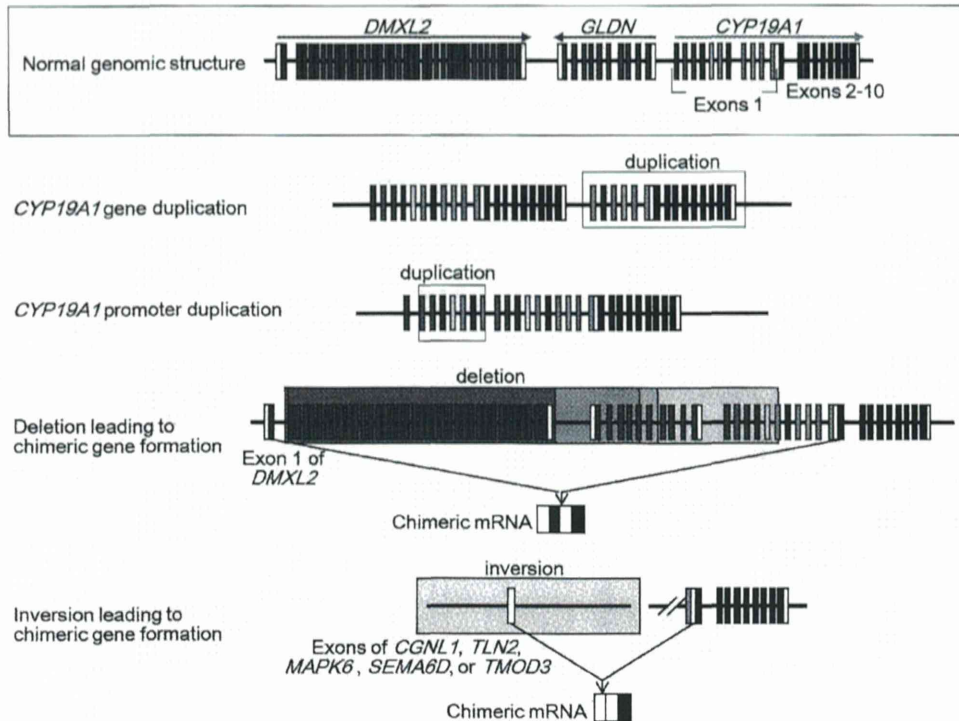


Figure 2: Underlying mechanisms of CYP19A1 overexpression. The arrows indicate genomic position and transcriptional direction of genes (5'>3'). For CYP19A1, the black and colored boxes indicate the coding exons 2-10 and non-coding exons 1, respectively. The white boxes in exons 2 and 10 depict untranslated regions. For other genes, the white and colored boxes indicate the untranslated and translated regions, respectively. Two simple duplications, four simple deletions, one complex deletion, two simple inversions, and three complex inversions have been identified. Of these, duplications include the promoter and/or coding regions of CYP19A1, while deletions and inversions create chimeric genes consisting of coding exons of CYP19A1 and promoter-associated exons of neighboring genes.

15q21,(3,4,9) simple deletions in family C and families D-F reported by Fukami et al. (4) were likely to arise from NAHR and NHEJ, respectively, while the remaining deletion, duplications, and complex rearrangements were consistent with RBE.(3,4,9) The underlying mechanisms for inversions have yet to be clarified. Notably, breakpoint-flanking regions of the rearrangements, except for that of a NAHR-mediated deletion, were not associated with known rearrangement-inducing DNA features.(9) Moreover, while structural alterations on the human genome are known to preferentially occur in late-replicating parts of the genome,(14) rearrangements at 15q21 were located within an early-replicating segment.(9) Thus, there may be hitherto unknown factors that contribute to genomic instability of the 15q21 region. In this regard, although the frequencies of repetitive sequences including Alus and LINES are relatively high in the breakpoint-flanking regions of

rearrangements at 15q21, (Figure 1) (9) it remains unknown whether these sequences are associated with the genomic alterations.

Clinical Manifestations of Patients with AEXS

To date, 30 male patients from 15 families with molecularly confirmed AEXS have been reported. (Table 1) (2-4,7,9) All probands were ascertained by pre- or peri-pubertal onset gynecomastia. (Figure 3) Additional clinical features included small testes, high-pitched voice, scarce facial hair, and variably advanced bone age. Genital appearance at birth and fertility in adulthood were normal, and male gender identity was preserved. The clinical features are explicable by estrogen excess resulting from CYP19A1 overexpression. Indeed, increased mRNA expression of CYP19A1 and enhanced enzymatic activity of aromatase were observed in skin fibroblasts obtained from patients.(4)

Phenotypes of female patients with AEXS have been poorly investigated. Most of these individuals seem to be asymptomatic, although macromastia, irregular menses, precocious puberty, and short adult height have been described in some cases.(3,4,6,7)

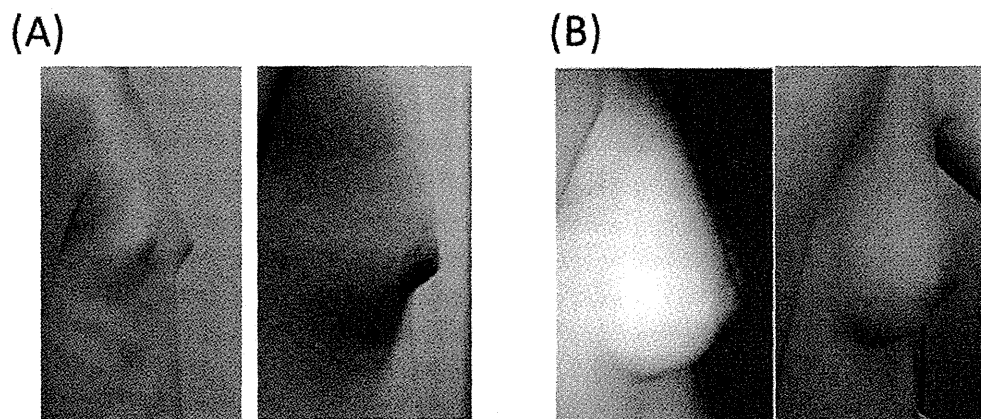


Figure 3: Gynecomastia in patients with AEXS. (A) Relatively mild gynecomastia in patients with duplications. (B) Moderate or severe gynecomastia in patients with deletions.

Hormonal Abnormalities in Male Patients with AEXS

Male patients with AEXS show FSH-dominant gonadotropin deficiency. (Table 2) (2,4,7-9) Serum FSH levels are low at baseline and poorly respond to GnRH stimulation, while LH levels are grossly normal at baseline and variably respond to GnRH stimulation. Serum testosterone (T) levels are usually normal or slightly reduced, while estradiol (E2) levels are normal or elevated. Blood E2/T ratios and estrone (E1) values are significantly increased. Sex hormone abnormalities are more apparent in patients with chimeric genes than in those with duplications, while the degree of gonadotropin deficiency is comparable among patients irrespective of the type of the rearrangements. These data imply that estrogens exert a negative feedback effect on gonadotropin secretion mainly at the pituitary level. Since FSH secretion is similarly affected in all patients, it appears that only mild excess of circulating estrogens is sufficient to suppress FSH secretion.

It is worth mentioning that serum E2 levels remained undetectable in previously reported pre- and early-pubertal boys with AEXS who showed clinically recognizable gynecomastia and markedly increased growth velocity. (Table 2) (7) Such clinical features in pre- and early-pubertal patients are unlikely to be associated with increased conversion of gonadal T into E2. It is possible that adrenal androgens such as androstenedione serve as the major sources of estrogens in children with AEXS, because adrenarche (increased production of adrenal steroids) occurs several years before the onset of puberty. (15) Indeed,

serum levels of E1, a metabolite of androstenedione, are significantly elevated in patients with AEXS. (4)

Genotype-Phenotype Correlation

The clinical severity of AEXS appears to be determined by functional and structural properties of the fused promoters and by copy-number of CYP19A1. (Table 1 and Figure 3) (4,9) First, patients with CYP19A1 duplication exhibit milder phenotypes than those with chimeric genes. These results can be explained by a tissue-limited expression pattern of CYP19A1 and broad expression patterns of other genes involved in chimeric gene formation, because the expression patterns of the chimeric genes are predicted to follow those of the original genes. Second, among the patients with chimeric genes, those with DMXL2-CYP19A1 genes manifest the mildest phenotype. These results are consistent with the presence of a transcription start site (ATG) in exon 1 of DMXL2 and the absence of such sites in the fused exons of the other five genes involved in chimeric gene formation. (Figure 2) It is likely that DMXL2-CYP19A1 chimeric mRNAs preferentially recognize the natural start codon on DMXL2 exon 1 and undergo nonsense-mediated mRNA decay, while other chimeric mRNAs exclusively utilize the start codon on CYP19A1 exon 2 and produce the aromatase protein. Third, phenotypic severity is variable among patients with simple deletions, although they are predicted to have the same DMXL2-CYP19A1 chimeric gene. The differences can be ascribed to the presence or absence of CYP19A1 promoters; patients with large deletions affecting the CYP19A1 promoters and DMXL2 exons show milder phenotypes

Aromatase Excess Syndrome

Table 1. Previously reported patients with aromatase excess syndrome.

Case/family	Number of patients*	Genomic rearrangement	Predicted mechanism for CYP19A1 overexpression	Fused promoter**
Case 1	1	Simple duplication	Gene duplication	...
Case 2	3***	Simple deletion	Chimeric gene formation	DMXL2
Case 3	1	Complex****	Chimeric gene formation	DMXL2
Case 4	1	Complex****	Chimeric gene formation	SEMA6D
Case 5	1	Complex****	Chimeric gene formation	TMOD3
Case 6	2	Complex****	Chimeric gene formation	CGML1
Families A-B	4	Simple duplication	Promoter duplication	...
Family C	2	Simple deletion	Chimeric gene formation	DMXL2
Families D-F	12	Simple deletion	Chimeric gene formation	DMXL2
Patient 1	1	Simple inversion?*****	Chimeric gene formation	TLN2
Family 2	1	Simple inversion?*****	Chimeric gene formation	MAPK6
Family	3	Simple deletion	Chimeric gene formation	DMXL2

Table 1. Previously reported patients with aromatase excess syndrome.

N.E., not examined; N.D., not described; SD, standard deviation.

* Number of male patients underwent clinical evaluation.

** Name of the gene that provides a cryptic promoter for CYP19A1.

*** Case 2 had a brother with gynecomastia and a father and several paternal relatives with advanced bone age and/or short stature.

**** Complex rearrangements with more than two breakpoints.

***** These inversions may be complex rearrangements, because copy-number analyses have not been performed for these cases/families.

Table 2. Hormonal data of male patients with aromatase excess syndrome.

Case	Case 1	Case 2	Case 3	Case 4
Age at examination (year)	10	18	15	13
Genomic rearrangement	Duplication	Deletion	Complex	Complex
At diagnosis*				
LH (mIU/mL)	<u><0.1</u> → 0.4 **		2.4	<u>1.3</u> → 24.9 **
FSH (mIU/mL)	<u>0.3</u> → 1.6 **		<1.0	<u>0.6</u> → 2.1 **
Testosterone (ng/dL)	<u>6</u> → 360 ***	260	70	150
Estrone (pg/mL)				111
Estradiol (pg/mL)	14.0	65.8	406.7	43.6
During AI treatment*				
LH (mIU/mL)	<u>0.5</u> → 7.3 **	44.8	4.7	
FSH (mIU/mL)	<u>1.7</u> → 3.2 **	34.9	<u>2.5</u>	
Testosterone (ng/dL)	90	860	690	
Estrone (pg/mL)				
Estradiol (pg/mL)	<10	6.4	13.1	

Table 2. Hormonal data of male patients with aromatase excess syndrome

AI, aromatase inhibitor

Hormonal values below the reference range are underlined, and those above the reference range are boldfaced.

* Hormone values are compared to age-matched male reference data.

** GnRH stimulation tests (100 µg/m², max. 100 µg bolus i.v.; blood sampling at 0, 30, 60, 90, and 120 minutes).

*** hCG stimulation tests (3000 IU/m², max 5000 IU i.m. for 3 consecutive days; blood sampling on days 1 and 4).

Conversion factors to SI units (multiply by): LH, 1.0 (IU/L); FSH, 1.0 (IU/L); testosterone, 3.467 (nmol/L); estrone, 3.699 (pmol/L); and estradiol, 3.671 (pmol/L).

Aromatase Excess Syndrome

Table 1. Previously reported patients with aromatase excess syndrome continued.

Onset of gynecomastia	Breast Tanner stage	Bone age advancement	Final height	Reference
7 years	2-3	Mild	Unknown	9
Unknown	1-3	Moderate	Unknown	9
8 years	4-5	N.E.	-0.9 SD	9
11 years	3-4	Moderate	Unknown	9
7 years	Severe	N.E.	<1 st percentile	2,9
5 years	Severe	N.E.	<1 st percentile	2,9
10-13 years	2-3	Mild	Normal	4
11-12 years	4	Mild/Moderate	Unknown	4
7-11 years	3-4	Moderate	~1.5 SD	4
N.D.	Severe	N.D.	Normal	3
8 years	Severe	Moderate	-1.5 SD	3
9 years	3-4	Moderate	-0.4 SD	7

Table 2. Hormonal data of male patients with aromatase excess syndrome continued..

Case	Case 5	Case 6	Proband	Brother	Father
	17	36	12	10	38
	Complex	Complex	Deletion	Deletion	Deletion
At diagnosis*					
	4.3	1.7	< 0.6	< 0.6	1.7
	2.7	1.5	2.3	< 0.4	1.6
	230	320	280	160	280
	556	903			
	392	223	< 25	< 25	49
During AI treatment*					
	8.9	2.9			
	5.6	5.6			
	530	1070			
	89	27.8			
	59	68.9			

Aromatase Excess Syndrome

than those with small deletions involving DMXL2 exons alone. (Figure 2) Lastly, other factors such as the physical distance between CYP19A1 and fused exons may also affect phenotypic severities of patients with chimeric genes.

Diagnosis and Management of AEXS

Patients with AEXS are usually ascertained by pre- or peri-pubertal onset gynecomastia. (2-4) AEXS seems to account a small number of cases of gynecomastia. Since no gene other than CYP19A1 has been implicated in autosomal dominant gynecomastia, a family history of gynecomastia is important for the clinical diagnosis of AEXS. However, sporadic cases with AEXS have been reported. (2-4,9) Furthermore, other environmental and genetic factors also underlie familial gynecomastia. (16) For example, mutations in the androgen receptor gene can result in familial gynecomastia with an X-linked inheritance pattern. (17) AEXS should be suspected when gynecomastia is associated with FSH-dominant gonadotropin deficiency, elevated serum E1 levels, and advanced bone age. For molecular diagnosis of AEXS, copy-number analysis using comparative genomic hybridization is useful, because rearrangements in AEXS are undetectable by standard karyotyping. (4,9) In addition, mRNA analysis may be necessary for copy-number neutral inversions. (2,3)

A unified management approach for patients with AEXS has not been fully established. Patients with mild phenotypes would not necessarily require medical intervention. Patients with obvious gynecomastia often undergo mastectomy. (2,4) Mastectomy has been shown to be effective for gynecomastia of various causes, including AEXS, although this treatment is associated with minor complications such as skin retraction, hypertrophic scars, hypoesthesia, and skin redundancy. (18) As a pharmacological intervention, anastrozole, a third-generation aromatase inhibitor that is commonly prescribed to females with breast cancer, has been used for a small number of patients with AEXS. (2,4) Anastrozole administration has ameliorated gynecomastia as well as hormonal abnormalities in all patients with AEXS treated so far. It seems that ≤ 1 mg/day is sufficient to improve clinical manifestations in patients with duplications and deletions, while 2-4 mg/day of anastrozole may be required for patients with inversions. (2,4) No adverse events during anastrozole treatment have been described in patients with AEXS, although long-term safety of this drug remains currently unknown.

Conclusions

AEXS is a rare example of a human congenital disorder caused by gene overexpression resulting from submicroscopic genomic rearrangements. AEXS should be included in the differential diagnosis of pre- or peri-pubertal onset gynecomastia. A positive family history, characteristic hormonal abnormalities, and advanced bone age are key features of AEXS. Further studies are necessary to determine the frequency of AEXS among patients with gynecomastia and to establish an optimal treatment strategy for this condition.

Acknowledgements

This work was supported by grants from the Ministry of Health, Labor and Welfare and from Takeda Science Foundation, by Grants-in-Aid for Scientific Research from the Japan Society for the Promotion of Science and from the Ministry of Education, Culture, Sports, Science and Technology, and by the Grant of National Center for Child Health and Development.

Disclosure

All authors declare no conflict of interest.

Maki Fukami MD
Mami Miyado PhD
Keisuke Nagasaki MD
Makio Shozu MD
Tsutomu Ogata MD

References

1. Bhasin S. Testicular disorders. In: Kronenberg HM, Melmed M, Polonsky KS, Larsen PR, eds. *Williams textbook of endocrinology*. 11th ed. Philadelphia: Saunders, 2011;645-699
2. Shozu M, Sebastian S, Takayama K, Hsu WT, Schultz RA, Neely K, Bryant M, Bulun SE. Estrogen excess associated with novel gain-of-function mutations affecting the aromatase gene. *N Engl J Med* 2003;348:1855-1865
3. Demura M, Martin RM, Shozu M, Sebastian S, Takayama K, Hsu WT, Schultz RA, Neely K, Bryant M, Mendonca BB, Hanaki K, Kanzaki S, Rhoads DB, Misra M, Bulun SE. Regional rearrangements in chromosome 15q21 cause formation of cryptic promoters for the CYP19 (aromatase) gene. *Hum Mol Genet* 2007;16:2529-2541
4. Fukami M, Shozu M, Soneda S, Kato F, Inagaki A, Takagi H, Hanaki K, Kanzaki S, Ohyama K, Sano T, Nishigaki T, Yokoya S, Binder G, Horikawa R, Ogata T. Aromatase excess syndrome: identification of cryptic duplications and deletions leading to gain of function of CYP19A1 and assessment of phenotypic determinants. *J Clin Endocrinol Metab*. 2011;96:E1035-1043
5. Binder G, Iliev DI, Dufke A, Wabitsch M, Schweizer R, Ranke MB, Schmidt M. Dominant transmission of prepubertal gynecomastia due to serum estrone excess: hormonal, biochemical, and genetic analysis in a large kindred. *J Clin Endocrinol Metab* 2005;90:484-492
6. Martin RM, Lin CJ, Nishi MY, Billerbeck AE, Latronico AC, Russell DW, Mendonca BB. Familial hyperestrogenism in both sexes: clinical, hormonal, and molecular studies of two siblings. *J Clin Endocrinol Metab* 2003;88:3027-3034
7. Shihara D, Miyado M, Nakabayashi K, Shozu M, Ogata T, Nagasaki K, Fukami M. Aromatase excess syndrome in a family with upstream deletion of CYP19A1. *Clin Endocrinol* 2013 (in press)
8. Fukami M, Shozu M, Ogata T. Molecular bases and phenotypic determinants of aromatase excess syndrome. *Int J Endocrinol* 2012;584807
9. Fukami M, Tsuchiya T, Vollbach H, Brown KA, Abe S, Ohts S, Wabitsch M, Burger H, Simpson ER, Umezawa A, Shihara D, Nakabayashi K, Bulun SE, Shozu M, Ogata T. Genomic basis of aromatase excess syndrome: Recombination- and replication-mediated rearrangements leading to CYP19A1 overexpression. *J Clin Endocrinol Metab* 2013 (in press)
10. Lupski JR, Stankiewicz P. Genomic disorders: molecular mechanisms for rearrangements and conveyed phenotypes. *PLoS Genet* 2005;1:e49
11. Hastings PJ, Ira G, Lupski JR. A microhomology-mediated break-induced replication model for the origin of human copy number variation. *PLoS Genet* 2009;5:e1000327
12. Gu W, Zhang F, Lupski JR. Mechanisms for human genomic rearrangements. *Pathogenetics* 2008;1:4
13. Shaw CJ, Lupski JR. Implications of human genome architecture for rearrangement-based disorders: the genomic basis of disease. *Hum Mol Genet* 2004;13:R57-64
14. Koren A, Polak P, Nemes J, Michaelson JJ, Sebat J, Sunyaev SR, McCarroll SA. Differential relationship of DNA replication timing to different forms of human mutation and variation. *Am J Hum Genet* 2012;91:1033-1040
15. Tung YC, Lee JS, Tsai WY, Hsiao PH. Physiological changes of adrenal androgens in childhood. *J Formos Med Assoc* 2004;103:921-924
16. Nordt CA, DiVasta AD. Gynecomastia in adolescents. *Curr Opin Pediatr* 2008;20:375-382
17. Hellmann P, Christiansen P, Johannsen TH, Main KM, Duno M, Juul A. Male patients with partial androgen insensitivity syndrome: a longitudinal follow-up of growth, reproductive hormones and the development of gynecomastia. *Arch Dis Child* 2012;97:403-409
18. Lawrence SE, Faught KA, Vethamuthu J, Lawson ML. Beneficial effects of raloxifene and tamoxifen in the treatment of pubertal gynecomastia. *J Pediatr* 2004;145:71-76

ORIGINAL ARTICLE

Copy-number variations in Y-chromosomal azoospermia factor regions identified by multiplex ligation-dependent probe amplification

Kazuki Saito^{1,2,3}, Mami Miyado¹, Yoshitomo Kobori⁴, Yoko Tanaka⁵, Hiromichi Ishikawa⁶, Atsumi Yoshida⁷, Momori Katsumi¹, Hidekazu Saito³, Toshiro Kubota², Hiroshi Okada⁴, Tsutomu Ogata^{1,8} and Maki Fukami¹

Although copy-number variations (CNVs) in Y-chromosomal azoospermia factor (AZF) regions have been associated with the risk of spermatogenic failure (SF), the precise frequency, genomic basis and clinical consequences of these CNVs remain unclear. Here we performed multiplex ligation-dependent probe amplification (MLPA) analysis of 56 Japanese SF patients and 65 control individuals. We compared the results of MLPA with those of conventional sequence-tagged site PCR analyses. Eleven simple and complex CNVs, including three hitherto unreported variations, were identified by MLPA. Seven of the 11 CNVs were undetectable by conventional analyses. CNVs were widely distributed in AZF regions and shared by ~60% of the patients and ~40% of the controls. Most breakpoints resided within locus-specific repeats. The majority of CNVs, including the most common *gr/gr* deletion, were identified in the patient and control groups at similar frequencies, whereas simple duplications were observed exclusively in the patient group. The results imply that AZF-linked CNVs are more frequent and heterogeneous than previously reported. Non-allelic homologous recombination likely underlies these CNVs. Our data confirm the functional neutrality of the *gr/gr* deletion in the Japanese population. We also found a possible association between AZF-linked simple duplications and SF, which needs to be evaluated in future studies.

Journal of Human Genetics advance online publication, 8 January 2015; doi:10.1038/jhg.2014.115

INTRODUCTION

Copy-number variations (CNVs) in azoospermia factor (AZF) a–c regions have been associated with the risk of spermatogenic failure (SF).^{1,2} Of these, submicroscopic deletions in AZFb and/or AZFc regions represent the major genetic causes of SF, although they are also observed in a small proportion of normozoospermic individuals.³ AZFb and AZFc regions are enriched with several locus-specific repeats and are highly susceptible to non-allelic homologous recombination.^{3,4} Deletions in these regions are predicted to cause SF by reducing the copy-number of multi-copy genes such as *DAZ*, *CDY1/2* and *TSPY1*.^{5–8} To date, deletions in AZFb/c regions were analyzed mostly by PCR of sequence-tagged site (STS) markers (STS-PCR).⁹ In 2011, Rozen *et al.*¹⁰ performed STS-PCR for 20 884 male individuals with and without SF and identified four types of AZFc deletions in 3.7% of the subjects. Rozen *et al.*¹⁰ revealed that most of these deletions exert negative effects on spermatogenesis; the most common deletion referred to as the *gr/gr* deletion almost doubled the risk of SF, whereas a deletion referred to as the *b2/b4* deletion increased the risk by a factor of 145. Other researchers have also

confirmed the pathogenicity of AZFb/c deletions.^{3,11} However, the frequencies and phenotypic effects of these deletions seem to differ among ethnic groups.^{11–13}

Other types of CNVs in AZF regions, such as microduplications and complex deletion–duplication rearrangements, have also been reported.^{14–18} However, the number of these reports is limited, because of technical difficulties in identifying such CNVs. Indeed, conventional STS-PCR has focused on deletions in AZFb and AZFc regions. Thus, the precise frequency, genomic basis and clinical consequences of AZF-linked CNVs remain largely unknown. For example, Giachini *et al.*¹⁸ found no significant pathogenic effect of AZFc duplications, whereas Lin *et al.*¹⁶ associated these duplications with a significant risk of oligospermia.

Recent advances in molecular techniques, including the development of multiplex ligation-dependent probe amplification (MLPA) and comparative genomic hybridization, have enabled researchers to identify CNVs at multiple loci in a single assay.^{19,20} In 2012, Bunyan *et al.*²¹ employed MLPA for the detection of CNVs in AZF regions. They studied 50 SF patients and 50 control individuals and identified

¹Department of Molecular Endocrinology, National Research Institute for Child Health and Development, Tokyo, Japan; ²Department of Comprehensive Reproductive Medicine, Tokyo Medical and Dental University, Tokyo, Japan; ³Division of Reproductive Medicine, Center for Maternal-Fetal-Neonatal and Reproductive Medicine, National Medical Center for Children and Mothers, Tokyo, Japan; ⁴Department of Urology, Dokkyo Medical University Koshigaya Hospital, Koshigaya, Japan; ⁵Department of Pediatrics, Tokyo Dental College Ichikawa General Hospital, Ichikawa, Japan; ⁶Reproduction Center, Tokyo Dental College Ichikawa General Hospital, Ichikawa, Japan; ⁷Reproduction Center, Kiba Park Clinic, Tokyo, Japan and ⁸Department of Pediatrics, Hamamatsu University School of Medicine, Hamamatsu, Japan
Correspondence: Dr M Fukami, Department of Molecular Endocrinology, National Research Institute for Child Health and Development, 2-10-1 Ohkura, Setagayaku, Tokyo 157-8535, Japan.
E-mail: fukami-m@ncchd.go.jp

Received 8 October 2014; revised 1 December 2014; accepted 6 December 2014

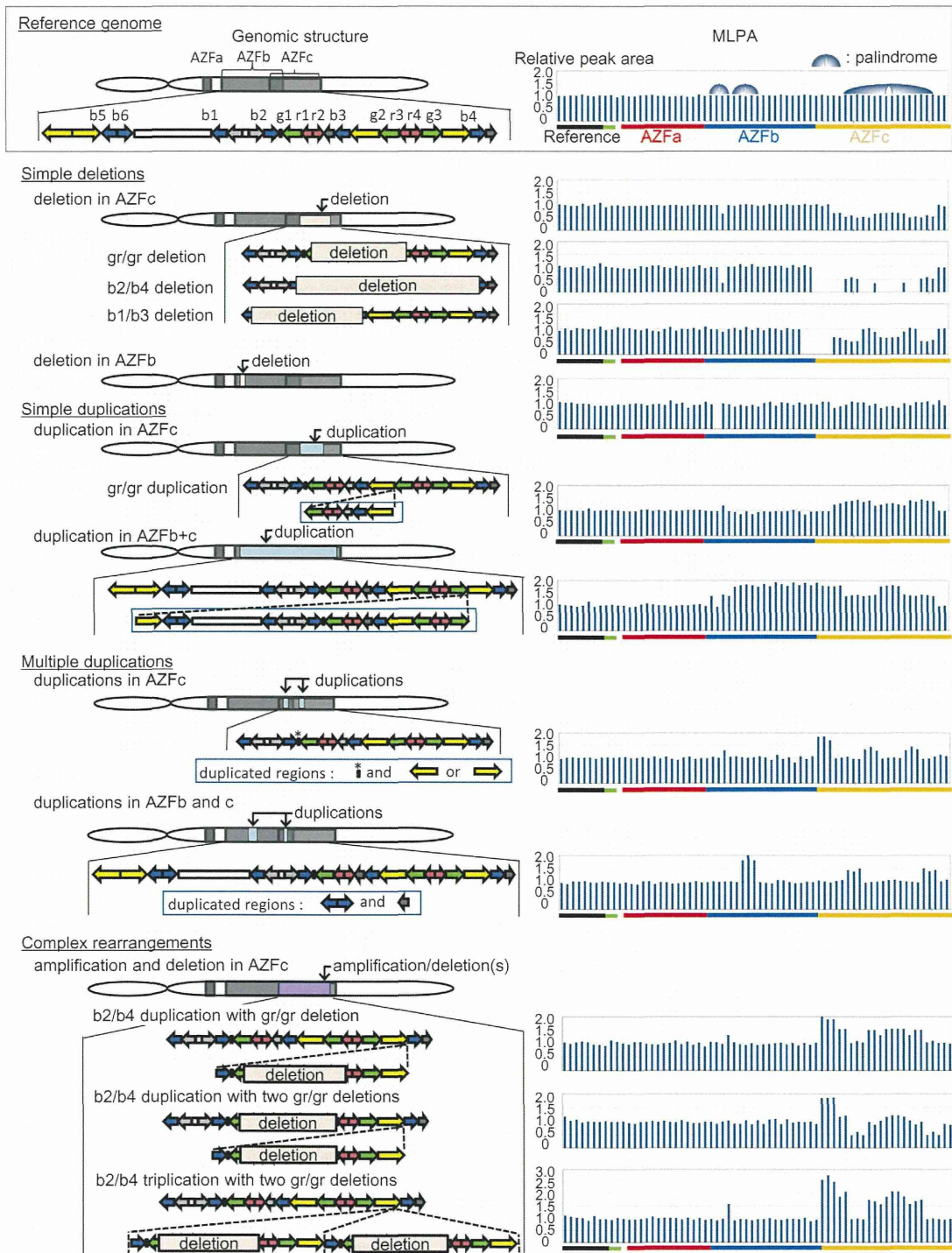


Figure 1 Copy-number variations in azoospermia factor (AZF) regions identified by multiplex ligation-dependent probe amplification (MLPA). Left panel: Schematic representation of the genomic structure of AZF regions. The colored arrows depict the locus-specific repeats in AZFb/c regions. The structure of the reference genome is based on the sequence retrieved from GenBank. Right panel: Representative results of MLPA. The relative peak areas were calculated by dividing each peak area of the samples by the average of that of five reference samples. Decreased and increased relative peak areas suggest copy-number loss and gain, respectively.

four types of simple CNVs that were undetectable by STS-PCR. Likewise, Liu *et al.*²² performed MLPA analysis of samples obtained from 199 fathers and their sons. Although Liu *et al.* identified AZF-linked deletions in 7.5% of the fathers, they did not analyze the presence or absence of copy-number gains. There have been no further reports of MLPA analysis for AZF regions. Here we performed MLPA on 121 Japanese individuals with and without SF.

SUBJECTS AND METHODS

Subjects

A total of 121 unrelated Japanese individuals participated in the present study. The patient group consisted of 56 men who were diagnosed with idiopathic non-obstructive azoospermia or oligospermia. All patients visited our clinics because of infertility. Patients with cytogenetically detectable chromosomal abnormalities were excluded from this study. The control group included 65 men who have fathered at least one child.

Molecular analysis

This study was approved by the Institutional Review Board Committee at the National Center for Child Health and Development and performed after taking written informed consent from the participants. Genomic DNA samples were obtained from peripheral leukocytes. MLPA was performed using SALSA MLPA probe-mix kit P360-A1 (MRC-Holland, Amsterdam, the Netherlands), according to the manufacturer's instructions. This kit contained 43 specific probes for AZF regions, together with 8 reference probes for other genomic regions (Supplementary Figure 1). The MLPA products were analyzed using a GenomeLab GeXP gene analysis system (Beckman Coulter, Fullerton, CA, USA). The relative peak area of each probe was calculated by dividing the actual peak area of the subject by the average of that of five reference samples. The results were confirmed by a second experiment.

To evaluate the usefulness of MLPA in the detection of AZF-linked CNVs, we compared the results of MLPA with those of conventional STS-PCR. In this study, five STS markers in AZFc region, sY1191, sY1291, sY1192, sY1189 and sY254, were analyzed as described previously.¹⁰

Statistical analysis

Statistical differences in the frequencies of CNVs between the patient and control groups were analyzed using χ^2 and Fisher's exact tests. Differences in the frequencies of copy-number gain of multi-copy genes were also analyzed using Fisher's exact tests. *P*-values <0.05 were considered significant.

RESULTS

Eleven types of CNVs were identified in 58 of the 121 individuals (Figure 1; Table 1). The 11 CNVs consisted of four simple deletions, two simple duplications, two multiple duplications (two non-overlapping duplications on one allele) and three complex rearrangements. The three complex rearrangements were assumed to be duplication or triplication of the genomic region between b2 and b4, which harbored the *gr/gr* deletion (Supplementary Figure 2). Most of the 11 CNVs involved genomic intervals in AZFc region, whereas two CNVs affected both AZFb and AZFc regions and one deletion involved only a small genomic interval in AZFb region. Three of the 11 CNVs, that is, a simple deletion in AZFb region, a simple duplication in AZFb+c region and multiple duplications in AZFb and AZFc regions, have not been reported previously. The breakpoints of 10 CNVs were located within AZF-specific repeats, whereas those of multiple duplications in AZFc region remained to be determined (Table 1).

Of the 11 CNVs detected by MLPA, only four were identified by STS-PCR (Figure 2). Three simple deletions in AZFc region (the *gr/gr*, b2/b4 and b1/b3 deletions) involving one or more of the five STS markers were detected by STS-PCR. One of the complex rearrangements (the b2/b4 duplication combined with *gr/gr* deletions) was assessed as a simple *gr/gr* deletion. Other CNVs, that is, a deletion in AZFb region, two of the three complex rearrangements and all duplications, yielded apparently normal results in STS-PCR.

Table 1 Copy-number variations identified in the present study

	Patient, n = 56	Control, n = 65	Statistical significance	Predicted position of the breakpoints		Estimated gene copy-number ^a				
				Proximal	Distal	DAZ (4)	CDY1 (2)	CDY2 (2)	HSFY (2)	USP9Y (1)
Any copy-number alteration	33	25	<i>P</i> =0.025							
Simple deletion	25	22	<i>P</i> =0.224							
<i>gr/gr</i> deletion	23	20		<i>gr</i> -repeat ^b	<i>gr</i> -repeat ^b	2	1	1	2	1
b2/b4 deletion	1	1		b2-repeat	b4-repeat	0	0	2	2	1
b1/b3 deletion	0	1		b1-repeat	b3-repeat	2	2	2	2	1
deletion in AZFb	1	0		y4-repeat	y4-repeat	4	2	1 or 2	2	1
Simple duplication	4	0	<i>P</i> =0.043							
<i>gr/gr</i> duplication	3	0		<i>gr</i> -repeat ^b	<i>gr</i> -repeat ^b	6	3	2	2	1
duplication involving AZFb+c	1	0		y3-repeat	y2-repeat	8?	3	3	4	1
Multiple duplications	1	1	<i>P</i> =0.713							
duplications in AZFc	1	0		Unknown	Unknown	4	3	2	2	1
duplications in AZFb and c	0	1		Repeat sequence ^c	Repeat sequence ^c	4	2	2	2 or 4	1
Complex rearrangements	3	2	<i>P</i> =0.331							
b2/b4 triplication with <i>gr/gr</i> deletions	1	0		Repeat sequence ^c	Repeat sequence ^c	8	4	2	2	1
b2/b4 duplication with <i>gr/gr</i> deletions	1	0		Repeat sequence ^c	Repeat sequence ^c	4	2	2	2	1
b2/b4 duplication with <i>gr/gr</i> deletion	1	2		Repeat sequence ^c	Repeat sequence ^c	6	3	2	2	1

^aThe numbers in the parentheses indicate copy-number of the genes in the human reference sequence.

^bThe breakpoints reside within *g*- or *r*-repeat sequences.

^cAll of the multiple breakpoints reside within repeat sequences.